JOC Article

Photoarylation/Alkylation of Bromonaphthols

Luca Pretali,[†] Filippo Doria,[†] Daniela Verga,[†] Antonella Profumo,[‡] and Mauro Freccero*,[†]

Dipartimento di Chimica Organica and Dipartimento di Chimica Generale, Università di Pavia, 27100 Pavia, Italy

mauro.freccero@unipv.it

Received April 21, 2008

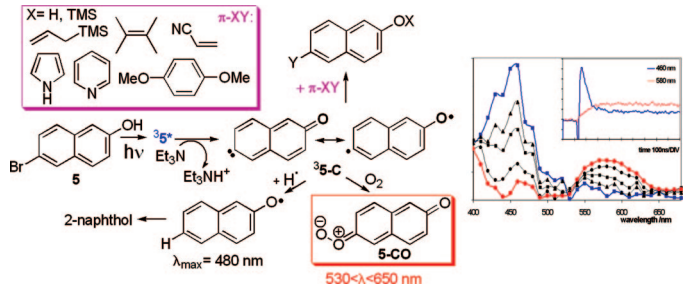

The photochemistry of 6-bromo-2-naphthols has been studied in acetonitrile, aqueous acetonitrile, and isopropyl alcohol in the absence and in the presence of triethylamine by product distribution analysis, laser flash photolysis (LFP), fluorescence, phosphorescence, electrochemical measurements, and DFT calculations. Hydrobromic acid loss in the presence of Et_3N occurs from the triplet state of 6-bromo-2-naphthol, generating an electrophilic carbene intermediate, which has been successfully trapped by oxygen, allyltrimethylsilane, 2,3-dimethylbut-2-ene, pyrrole, acrylonitrile, 1,4-dimethoxybenzene, and also pyridine. The generation and the reactivity of a triplet carbene intermediate has been supported by LFP, with the detection of 2,6-naphthoquinone-*O*-oxide ($530 < \lambda < 650$ nm) in the presence of O_2. The electrophilic diradical character of the carbene has been supported by DFT calculations, using the B3LYP, PBE0, and MPWB1K functionals, with the 6-31+G(d,p) basis set and PCM solvation model.

Introduction

The photochemistry of aromatic halides has been a hot issue for more than 40 years.[1] The carbon−halogen bond cleaving process, which is triggered by photoexcitation in solution, has been investigated by product distribution analysis[2] and laser flash photolysis detection (LFP)[3] and exploited for both synthetic purposes[2] and mild degradation of organic pollutants in water.[4] Mechanistic investigations, which have been stimulated by environmental issues, identify three main reaction pathways: (i) homolysis,[5] (ii) electron transfer, followed by cleavage of the resulting radical anion,[6] and (iii) heterolysis with the generation of an aryl cation as intermediate.[7]

$$\text{Ar-X}^* \rightarrow \text{Ar}^\bullet + \text{X}^\bullet \quad \text{(i)}$$

$$\text{Ar-X}^* \rightarrow (\text{Ar-X})^{\bullet -} \rightarrow \text{Ar}^\bullet + \text{X}^- \quad \text{(ii)}$$

$$\text{Ar-X}^* \rightarrow \text{Ar}^+ + \text{X}^- \quad \text{(iii)}$$

More recently, reaction mechanism iii has found synthetic application by Albini's group[8,9] in the formation of new aryl-

[†] Dipartimento di Chimica Organica.
[‡] Dipartimento di Chimica Generale.

(1) Grimshaw, J.; De Silva, A. P. *Chem. Soc. Rev.* **1981**, *10*, 181–203.
(2) Protti, S.; Fagnoni, M.; Mella, M.; Albini, A. *J. Org. Chem.* **2004**, *69*, 3465–3473.
(3) (a) Grabner, G.; Richard, C.; Köhler, G. *J. Am. Chem. Soc.* **1994**, *116*, 11470–11480. (b) Bonnichon, F.; Richard, C.; Grabner, G. *Chem. Commun.* **2001**, 73–74. (c) Bonnichon, F.; Grabner, G.; Guyot, G.; Richard, C. *J. Chem. Soc., Perkin Trans. 2* **1999**, 1203–1210. (d) Arnold, B. R.; Scaiano, J. C.; Bucher, G. F.; Sander, W. *J. Org. Chem.* **1992**, *57*, 6469–6474.
(4) Skurlatov, Y. I.; Ernestova, L. S.; Vichutinskaya, E. V.; Samsonov, D. P.; Semenova, I. V.; Rodko, I. Y.; Shvidky, V. O.; Pervunina, R. I.; Kemp, T. J. *J. Photochem. Photobiol. A* **1997**, *107*, 207–213.
(5) (a) Park, Y.-T.; Song, N. W.; Kim, Y.-H.; Hwang, C.-G.; Kim, S. K.; Kim, D. *J. Am. Chem. Soc.* **1996**, *118*, 11399–11405. (b) Grimshaw, J.; De Silva, A. P. *J. Chem. Soc.* **1979**, 193–194. (c) Grimshaw, J.; De Silva, A. P. *J. Chem. Soc., Chem. Commun.* **1980**, 302–303. (d) Grimshaw, J.; De Silva, A. P. *Can. J. Chem.* **1980**, *58*, 1880–1888.
(6) (a) Takeda, N.; Poliakov, P. V.; Cook, A. R.; Miller, J. R. *J. Am. Chem. Soc.* **2004**, *126*, 4301–4309. (b) Costentin, C.; Robert, M.; Savéant, J.-M. *J. Am. Chem. Soc.* **2004**, *126*, 16051–16057. (c) Chami, Z.; Gareil, M.; Pinson, J.; Saveant, J.-M.; Thiebault, A. *J. Org. Chem.* **1991**, *56*, 586–595. (d) Bunce, N. J.; Pilon, P.; Ruzo, L. O.; Sturch, D. J. *J. Org. Chem.* **1976**, *41*, 3023–3025.
(7) (a) Manet, I.; Monti, S.; Grabner, G.; Protti, S.; Dondi, D.; Dichiarante, V.; Fagnoni, M.; Albini, A. *Chem. Eur. J.* **2008**, *14*, 1029–1039. (b) Dichiarante, V.; Fagnoni, M.; Mella, M.; Albini, A. *Chem. Eur. J.* **2006**, *12*, 3905–3915.
(8) Protti, S.; Fagnoni, M.; Albini, A. *Org. Biomol. Chem* **2005**, *3*, 2868–2871.

10.1021/jo802374r CCC: $40.75
Published on Web 01/05/2009

SCHEME 1. Photogeneration of 4-Oxocyclohexa-2,5-dienylidene Carbene (3) and 4-Hydroxyphenyl Cation (4) from Chlorophenol 1 and Chloroanisole 2

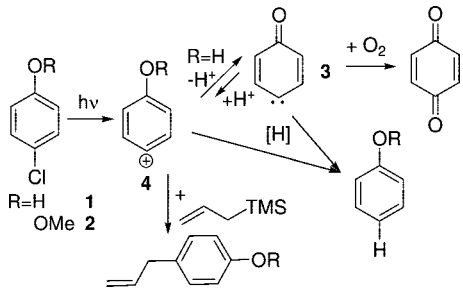

SCHEME 2

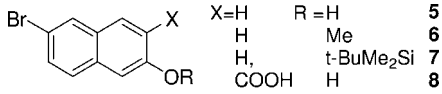

aryl and aryl-alkyl bonds. Among aryl halides, halophenols have been intensively investigated. In more detail, the photoreactivity of 4-chlorophenol (**1**) and derivatives (such as **2**) has been rationalized as the result of a heterolytic process involving 4-oxocyclohexa-2,5-dienylidene carbene (**3**)[3] and 4-hydroxyphenyl cation (**4**) (Scheme 1).[2] The carbene **3** arises from a deprotonation process of the 4-hydroxyphenyl cation, which has successfully been trapped by several π-nucleophiles, including allyltrimethylsilane.[2] Benzoquinone is the diagnostic trapping product of the carbene **3**, in the presence of oxygen. Despite the great effort toward mechanistic clarification and synthetic development related to such a photochemistry, only the reactivity of 4-chlorophenol (**1**) and 4-chloroanisole (**2**) has been thoroughly investigated and no reactivity data on halonaphthols are present, to our knowledge.

The above aspects, conjugated with the current interest of our group in the photoreactivity of binol-derivatives,[10] had prompted us to explore the photochemistry of several 6-bromo-2-naphthols and binol analogues. In this work, we describe the photochemistry of the 6-bromo-2-naphthols **5**−**8** (Scheme 2) in the presence of alkenes and aromatics to assess whether the reactivity of the resulting transient species may be exploited for the synthesis of functionalized naphthols.

In addition we have undertaken a parallel investigation aimed to clarify the nature and the properties of the reactive excited states and the further transients generated upon excitation of 6-bromo-2-naphthols by means of nanosecond laser flash photolysis (LFP), fluorescence, phosphorescence, and electrochemical measurements. The mechanistic aspects of the reaction have been supported by DFT calculation using the functionals B3LYP,[11] PBE0 (also known as PBE1PBE),[12] and MPWB1K[13] with 6-31G+(d,p) basis set, coupled with PCM solvation model, in order to reproduce the acetonitrile solvation effects.

SCHEME 3. Photoreactivity of 6-Br-2-naphthol (5), in the Presence of Allyltrimethylsilane (X = TMS), Pyrrole, 2,3-Dimethyl-2-butene, Acrylonitrile, Pyridine, and 1,4-Dimethoxybenzene (X = H)

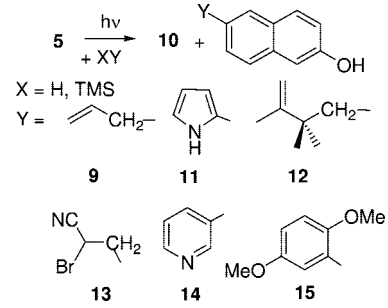

Results and Discussion

Photoreactivity of 6-Br-2-naphthol: Effects of the Solvents, Oxygen, and Allyltrimethylsilane. The photoreactivity of **5** was first explored in 2×10^{-3} M solutions using four lamps (15 W) centered at 310 nm, followed by chromatographic separation for the structural identification of the products. The reaction was initially carried out in the presence of allyltrimethylsilane ($1-5 \times 10^{-2}$ M), in several solvents: MeOH, isopropyl alcohol (IPA), acetonitrile (ACN), and aqueous ACN (H_2O/ACN = 7:3). In neat ACN and in polar protic solvents such as MeOH and IPA the reactant was recovered unmodified. Since allyltrimethylsilane is known to be one of the most efficient π-nucleophile traps for aryl cation intermediates, its generation as intermediate was doubtful.[14] In preparative irradiation experiments in argon-flushed aqueous ACN, the main isolated product was 6-allyl-2-naphthol (**9**) in fairly good yield (47%), together with 2-naphthol (**10**, 15% yield) and unreacted **5** (38%) (Scheme 3). However, in oxygen-equilibrated aqueous ACN no reactivity was detected. This fact, together with the evidence discussed in the next chapter, supports the proposal that reactivity may occur from the triplet excited state of **5** (^{3}**5***).

In an attempt to buffer the photogenerated acidity (by HBr), which may induce polymerization, isomerization, or hydrolysis of electron-rich π-nucleophiles (such as pyrrole and vinyl ethers) and the resulting adducts, the irradiations were also run in the presence of Et_3N (2×10^{-3} M), in neat and aqueous ACN and also in IPA. Surprisingly, the addition of Et_3N to an ACN solution of allyltrimethylsilane (2×10^{-2} M) and **5** (2×10^{-3} M) switched on the reactivity with a quantitative conversion of **5** into **9** in higher yield (70% yield) and **10** (30% yield). An almost identical conversion was achieved also in aqueous ACN with Et_3N. The addition of Et_3N to neat IPA afforded a quantitative conversion to **10** by a clean reductive dehalogenation process. In the presence of allyltrimethylsilane ($1-5 \times 10^{-2}$ M) beside **10** (96%) we also detected **9** in trace amounts (4% yield, by HPLC). The reaction was also carried out in the presence of Et_3N (6×10^{-3} M) in air-equilibrated neat ACN, with and without allyltrimethylsilane. In the absence of allyltrimethylsilane, 2,6-dihydroxynaphthalene (35% yield) and **10** (22% yield), together with unreacted **5** (25% yield), were isolated after reductive workup, using $Na_2S_2O_4$ and column chromatography separation. In the presence of allyltrimethylsilane, under the very same conditions, 2,6-dihydroxynaphtha-

(9) (a) Fagnoni, M.; Albini, A. *Acc. Chem. Res.* **2005**, *38*, 713–721. (b) Protti, S.; Fagnoni, M.; Albini, A. *Angew. Chem., Int. Ed.* **2005**, *44*, 5675–5678.

(10) (a) Colloredo-Mels, S.; Doria, F.; Verga, D.; Freccero, M. *J. Org. Chem.* **2006**, *71*, 3889–3895. (b) Richter, S. N.; Maggi, S.; Colloredo-Mels, S.; Palumbo, M.; Freccero, M. *J. Am. Chem. Soc.* **2004**, *126*, 13973–13979. (c) Doria, F.; Richter, S. N.; Nadai, M.; Colloredo-Mels, S.; Mella, M.; Palumbo, M.; Freccero, M. *J. Med. Chem.* **2007**, *50*, 6570–6579.

(11) (a) Becke, A. D. *J. Chem. Phys.* **1993**, *98*, 1372–1377. (b) Schmider, H. L.; Becke, A. D. *J. Chem. Phys.* **1998**, *108*, 9624–9631.

(12) (a) Adamo, C.; Barone, V. *J. Chem. Phys.* **1999**, *110*, 6158–6170. (b) Cimino, P.; Gomez-Paloma, L.; Barone, V. *J. Org. Chem.* **2004**, *69*, 7414–7422.

(13) Zhao, Y.; Truhlar, D. G. *J. Phys. Chem. A* **2005**, *109*, 5656–5667.

(14) (a) Milanesi, S.; Fagnoni, M.; Albini, A. *Chem. Commun.* **2003**, 216–217. (b) Manet, I.; Monti, S.; Fagnoni, M.; Protti, S.; Albini, A. *Chem. Eur. J.* **2005**, *11*, 140–151.

TABLE 1. Product Distribution from the Irradiation (λ = 310 nm) of 5 in ACN and Et_3N (2×10^{-2} M) in the Presence of Alkenes and Aromatics

XY[a]	conversion[b] (%)	products[c] (% yield)
a	92	**10** (32)
b	98	**11** (83), **10** (4)
c	100	**10** (92)
d	100	**9** (70), **10** (30)
e	95	**12** (38), **10** (40)
f	90	**13** (16), **10** (10)
g	78	**14** (30), **10** (2)
	96[d]	**14** (92), **10** (−)[d]
h	95	**15** (70), **10** (20)

[a] Irradiation time 1 h, T = 30 °C, [**5**] = 2×10^{-3} M, [Et_3N] = 2×10^{-3} M, [NuX] = $1-5 \times 10^{-2}$ M; **a**: morpholine; **b**: pyrrole; **c**: EVE; **d**: allyltrimethylsilane; **e**: 2,3-dimethyl-2-butene; **f**: acrylonitrile; **g**: pyridine. **h**: 1,4-dimethoxybenzene. [b] Reactant consumption. [c] The product yields have been determined after isolation by column chromatography (cyclohexane/ethyl acetate as eluent) or HPLC measurements. [d] Irradiation in neat pyridine in the absence of Et_3N.

lene (18% yield), **10** (41% yield), and **9** (19% yield) were detected by HPLC.

Photoreactivity of 6-Br-2-Naphthol in the Presence of Alkenes and Aromatics. We next investigated the photoreactivity of the naphthol **5** in ACN solution in the presence of Et_3N (2×10^{-3}M) and several traps (XY: n-,π-nucleophiles and radical traps, $1-5 \times 10^{-2}$ M) such as morpholine (**a**), pyrrole (**b**), ethyl vinyl ether (**c**, EVE), allyltrimethylsilane (**d**), 2,3-dimethyl-2-butene (**e**), acrylonitrile (**f**), pyridine (**g**), and 1,4-dimethoxybenzene (**h**). Naphthol **5** was reductively debrominated to **10** in the presence of morpholine and EVE but was converted into alkylated/arylated products (Scheme 3) in the presence of pyrrole, 2,3-dimethyl-2-butene, acrylonitrile, pyridine, and 1,4-dimethoxybenzene, in modest to fairly good yields (Table 1).

The formation of both the debrominated adduct **10** and the alkylation/arylation adducts **9**, **11**, **12**, and **15** at first glance suggests a behavior similar to that of 4-chlorophenol, which has been demonstrated to give adducts via both the corresponding phenyl cation **4** and carbene **3** in rapid equilibrium.[2,3] However, several aspects of this reaction, in particular, (i) the lack of reactivity in neat MeOH and IPA in the presence of allyltrimethylsilane, (ii) the reactivity in aqueous ACN and its quenching by the oxygen, (iii) the reactivity with acrylonitrile and pyridine, and above all (iv) the key role of Et_3N on the reactivity in neat ACN, suggest a slightly different scenario.

6-Br-2-naphthol Ethers. To understand the role of the phenol-like proton in the reaction, the photoreactivity of both methyl and silyl ethers was investigated. 2-Bromo-6-methoxynaphthalene **6** and (6-bromonaphthalen-2-yloxy)-*tert*-butyldimethylsilane **7** were chosen. Both **6** and **7** are photostable in MeOH, IPA, and aqueous ACN, in the presence of allyltrimethylsilane, since the starting material was quantitatively recovered after 2 h of irradiation. The lack of reactivity of both **6** and **7**, in comparison to that of **5**, both in aqueous ACN and in neat ACN containing Et_3N, suggests that the presence of the free hydroxyl group is mandatory for preserving the arylation/alkylation reactivity shown by **5**. This rules out an aryl cation as intermediate, since the chemical behavior of both **6** and **7** is very different from that of 4-chloroanisole.[7a] Such a conclusion is strengthened by the fact that with **5** alkylation/arylation occurs, although with a lower yield, also with acrylonitrile (16% conversion) and pyridine (30% yield in the presence of Et_3N; 92% yield in neat pyridine). With these traps, unidentified oligomeric byproducts were always recovered. The regiochemistry of the reaction leading to the adduct **13** was unambiguously established by DEPT, NOESY, and HMBC experiments. Arylation of pyridine at C3 yielding **14** was supported by the pattern of the aromatic protons of the pyridine moiety in the ^{1}H NMR spectra and by COSY experiments (see Supporting Information).

SCHEME 4. Photoreactivity of 8

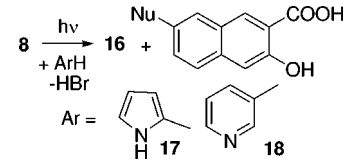

TABLE 2. Product Distribution from the Irradiation of 8 in Neat Acetonitrile (with Et_3N) and in Aqueous Buffered Conditions

XY[a]	conditions (λ = 360 nm)[b]	consumption (%)	products[c] (% yield)
a	**8** + Et_3N, CH_3CN	75	**16** (52), **17** (20)
	8 H_2O, pH 9.0[d]	42	**16** (22), **17** (16)
	8 H_2O/CH_3CN = 1:1, pH 7.8[d]	15	**16** (5), **17** (5)
g	**8** H_2O/CH_3CN = 1:1, pH 9.0[d]	90	**16** (57), **18** (21)

[a] **a**: pyrrole; **g**: pyridine. [b] Irradiation time 1 h, T = 30 °C, [**8**] = 2×10^{-3} M, [Et_3N] = 4×10^{-3} M, [NuX] = $1-5 \times 10^{-2}$ M. [c] The product yields have been determined after isolation by reverse column chromatography RP C18 ($MeOH/H_2O$ = 1:1 as eluent). [d] Buffered conditions.

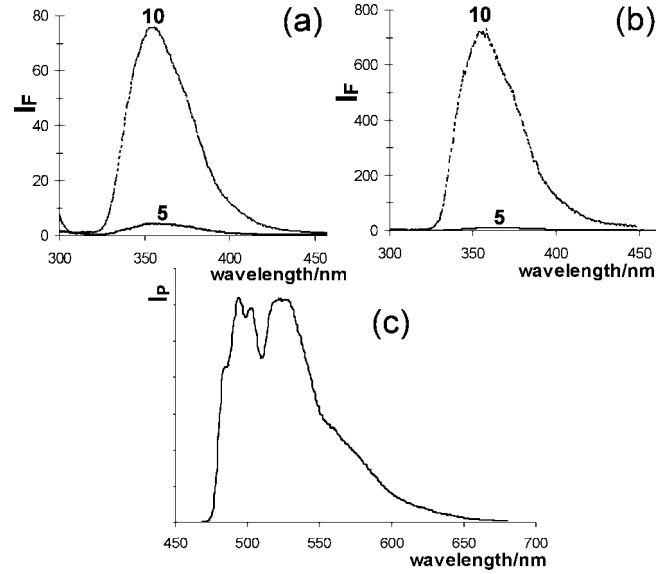

FIGURE 1. Fluorescence emission spectra of **5** and **10** in neat ACN (a) and in aqueous ACN (b). Excitation wavelength set at 290 nm. (c) Phosphorescence spectrum of **5** in EPA (diethyl ether/isopentane).

Photoreactivity of a Water-Soluble 6-Br-2-naphthol. Irradiation of the naphthalene carboxylic acid **8** at 360 nm in the presence of pyrrole and pyridine in neat acetonitrile with Et_3N and in buffered aqueous acetonitrile (pH 9) afforded the adducts **17** and **18**, respectively, together with the debrominated product **16**, which became the main product (Scheme 4). The process is more efficient in neat acetonitrile and under basic aqueous solution (pH 9) than in aqueous acetonitrile at pH 7.8 (Table 2).

Fluorescence and Phosphorescence Measurements. The fluorescence emission spectra of **5** and **10** (both 10^{-5} M) are shown in Figure 1. The emission maxima are centered at λ_{max} = 358 nm for naphthol **10** and 372 nm for **5**. The decrease in fluorescence intensity passing from **10** to the Br-naphthol **5** is

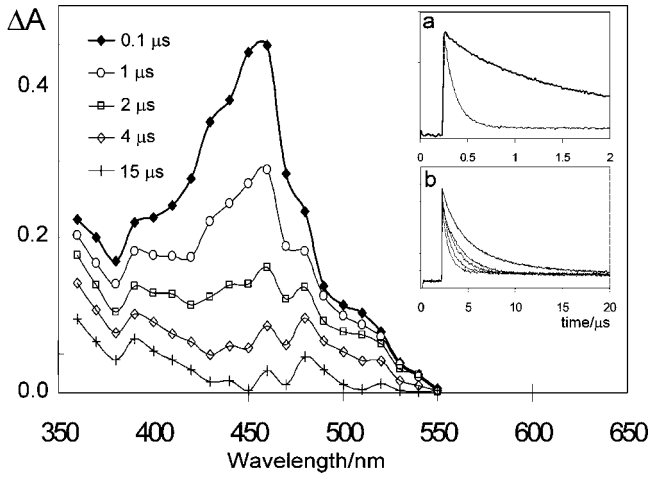

FIGURE 2. Transient absorption spectra of **5** in acetonitrile. The spectra were taken 0.1, 1, 2, 4, and 15 μs after the laser pulse, respectively. Inset a shows the decay traces with O_2 (fine line) and without (thicker line), monitored at 460 nm. Inset b shows the decay traces without and with Et_3N (3×10^{-4}, 6×10^{-4}, 2×10^{-3}, 3×10^{-3} M, respectively), monitored at 460 nm.

remarkable in both neat ACN (Figure 1a) and in aqueous ACN (Figure 1b). These results can be interpreted in terms of an internal heavy-atom effect, which should increase the intersystem crossing (ISC) efficiency. In addition, the fluorescence of both **5** and **6** is not quenched by Et_3N (2×10^{-2} M) in ACN solution, and it does not change by more than 10% passing from neat ACN to aqueous ACN. The above evidence together with the lack of reactivity in air-equilibrated aqueous ACN (without Et_3N) discussed above suggest that the triplet state could be involved in the reactivity of **5**. Therefore, the phosphorescence spectrum of 6-bromo-2-naphthol was recorded in EPA (diethyl ether/isopentane) glassy matrices at 77 K to evaluate its energy. From the onset of the spectrum (Figure 1c) it has been possible to evaluate the energy of ^{3}**5*** ($E_{0,T}$ = 60.5 kcal mol^{-1}).

Laser Flash Photolysis Studies: Generation and Quenching of ^{3}5*. The photoactivation processes of **5** have also been studied by laser flash photolysis (LFP), with the aim to clarify (i) the nature of the excited state involved and (ii) the role of the Et_3N and (iii) to detect further transient species. Indeed, LFP of **5** at 266 nm (4 mJ/pulse, Nd:YAG laser) in neat ACN and aqueous ACN (pH 7, buffered conditions) yielded an intense transient absorbance centered at λ_{max} = 460 nm, which was efficiently quenched by O_2 (Figure 2, inset a).

Therefore, based also on the spectroscopic similarity of triplet excited state of **10** (^{3}**10***) (λ_{max} = 430 nm),[15] the above transient has been attributed to ^{3}**5***. The intensity of the end of pulse signals assigned to the triplets of the Br-naphthols **5**−**7** is at least 10-fold higher than that of ^{3}**10***. This result is consistent with the fluorescence measurements, suggesting that for the Br-naphthols **5**−**7**, the singlet state is converted into the triplet by rapid ISC. The profile of such a transient absorbance follows mainly a second-order decay in the absence of O_2 in neat ACN (Figure 2, inset a, darker line), and in aqueous ACN it is slightly faster. The decay became a pseudo-first-order upon addition of Et_3N, in the concentration range 3×10^{-4}−3×10^{-3} M (Figure 2, inset b), with a $k_2 = 9.0(\pm 1.0) \times 10^7$ M^{-1} s^{-1} and without significant bleaching of the transient signal after the laser shot. The latter evidence, together with the lack of fluorescence quenching caused by Et_3N ($\leq 2 \times 10^{-2}$ M), suggests that the amine acts as a triplet rather than a singlet quencher. In addition, a very similar transient has been recorded also for the methyl and TBS ethers (**6** and **7**, respectively).

In contrast, the lifetimes of the triplet states ^{3}**6*** and ^{3}**7*** were not significantly affected by Et_3N addition. These LFP data, together with the photoreactivity of **5** in neat ACN in the presence of Et_3N and the effect of the oxygen on the photoreactivity in aqueous ACN discussed above, suggest that (i) Et_3N reacts with the triplet excited state and (ii) the reactivity could be triggered by a deprotonation process of the naphthol in the triplet excited state. The quenching of ^{3}**5*** by Et_3N should not be ascribed to a photoinduced electron transfer (PET) process, since when the naphthol OH is protected, no significant lifetime reduction of the triplet excited state (^{3}**6*** and ^{3}**7***) was recorded.

Electrochemical Measurements. To rule out the mechanism of photoinduced electron transfer (PET) from Et_3N to ^{3}**5***, we had to measure the reduction potential of **5** and **6** by cyclic voltammetry. Typical voltammograms of **5** in ACN 0.1 M nBu$_4$PF$_6$ have been measured using glassy carbon disk electrode versus Ag/AgCl. The reduction waves for the naphthols **5** and **6** were always chemically irreversible using scan rates from 100 to 1300 mV s^{-1}, without the formation of anodic peaks. The cathodic peak potentials [$E_{pc} - E_{red}$(**5**)] measured using a scan rate of 100 mV s^{-1} were similar: −2.29 and −2.40 V for **5** and **6** respectively. Using the literature oxidation potential of Et_3N in ACN [$E_{ox}(Et_3N)$, +1.19 V vs NHE; +0.991 V vs Ag/AgCl in ACN][16] and the energy of ^{3}**5*** [$E(^3$**5***), evaluated from phosphorescence measurements], we have been able to estimate the PET as strongly endoergonic by 15 kcal/mol, using eq 1:

$$\Delta G_{et} = 23.06[E_{ox}(Et_3N) - E_{red}(5)] - E(^3\mathbf{5}^*) \qquad (1)$$

Therefore, the PET mechanism cannot play a significant role in the quenching of ^{3}**5*** by Et_3N, as supported by the evidence that ^{3}**6*** lifetime does not change in ACN in the presence of the amine.

Further Laser Flash Photolysis Studies: Detection of Transients Arising from ^{3}5*. Photolysis of an air-equilibrated solution of **5** in ACN in the presence of Et_3N (5×10^{-2} M), immediately after the pulse produces a spectrum similar to that of Figure 2. After decay of the triplet signal, a long-lived absorption ($t_{1/2}$ > 20 μs) with a broad absorption band from 540 to 650 nm remains (Figure 3). Such a new transient species is formed only in the presence of O_2. The inset of Figure 3 displays a rising time at 580 nm, which parallels the decay of ^{3}**5*** at 460 nm. These traces suggest a sequential generation of the new species starting from ^{3}**5***. Grabner's group has shown that **3** in its triplet state (^{3}**3-C**), generated from the photolysis of **1** (Scheme 5), reacts with oxygen yielding benzo-1,4-quinone-*O*-oxide (^{1}**3-CO**).[3a,b] This latter species exhibits a broad absorption band (420−580 nm) with a maximum centered at 460 nm (Scheme 5).[3a,d] Therefore, taking also into consideration that **5**exhibits a more extended conjugation in comparison to **1**, we believe that the transient with absorbance from 530 to 650 nm may be assigned to the carbonyl oxide ^{1}**5-CO**. This intermediate is generated in the trapping reaction of the triplet carbene ^{3}**5-C** by molecular oxygen, and further ISC (Scheme 5). This rationalization agrees with the product analysis in the preparative irradiation in the presence of O_2, with generation of 2,6-dihydroxynaphthalene, after reductive workup.

(15) Kleinman, M. H.; Flory, J. H.; Tomalia, D. A.; Turro, N. J. *J. Phys. Chem. B* **2000**, *104*, 11472–11479.

(16) Liu, W.-Z.; Bordwell, F. G. *J. Org. Chem.* **1996**, *61*, 4779–4783.

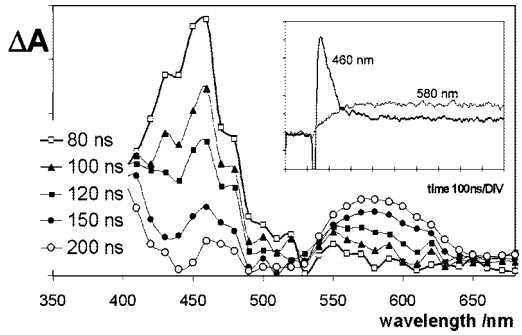

FIGURE 3. Transient absorption spectra of **5** in ACN with Et_3N (5×10^{-2} M), in the presence of O_2 (air-equilibrated solution). The spectra were taken 80, 100, 120, 150, and 200 ns after the laser pulse, respectively. The inset shows the decay traces monitored at 460 and 580 nm.

SCHEME 5. Parallel Photoreactivity of 1 and 5

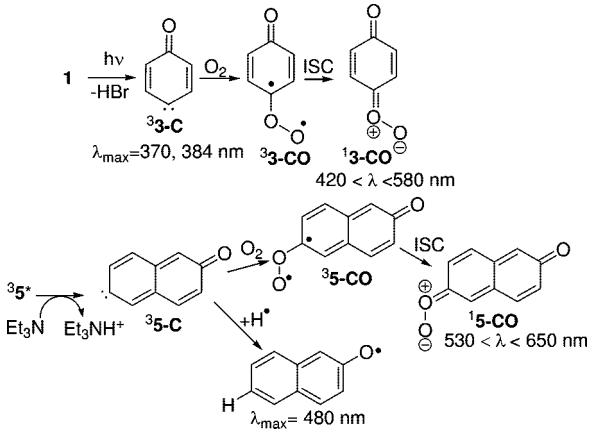

Flash photolysis of **5** in deoxygenated ACN in the presence of Et_3N (4×10^{-2} M) leads to the appearance of another transient with an absorption spectra blue-shifted in comparison to that of ^{1}**1-CO** ($\lambda_{max} = 480$ nm, Figure 4). This transient is in excellent agreement with the reported spectrum of 2-naphthoxyl radical,[17] which should arise from the carbene ^{3}**5-C**, by hydrogen abstraction. This transient decays with a pseudo-first-order kinetic, exhibiting a lifetime dependent on Et_3N concentration ($k_2 = 9.2 \times 10^5$ $M^{-1}s^{-1}$). We were unable to directly detect the carbene ^{3}**5-C** in the presence of Et_3N. These LFP data seem to support the conclusion that the observed reactivity of **5** in the presence of Et_3N has to be ascribed to the carbene intermediate ^{3}**5-C**.

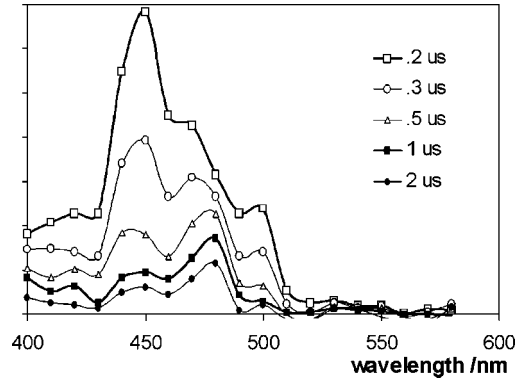

FIGURE 4. Transient absorption spectra of **5** in ACN with Et_3N (4×10^{-2} M), in the absence of O_2 (Ar-equilibrated solution). The spectra were recorded 0.2, 0.3, 0.5, 1, and 2 μs after the laser pulse.

SCHEME 6. Isodesmic Reactions Used To Calculate the pK_a of ^{3}5* at R(U)B3LYP/6-31+G (d,p) Level of Theory and UAHF Radii in Aqueous Solution

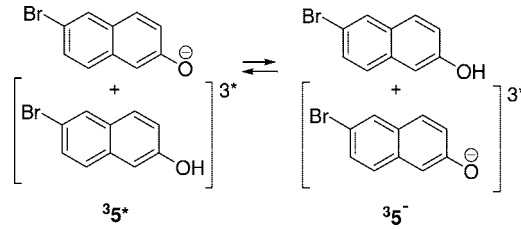

DFT Calculations: Properties and Reactivity of the Transients. To gather additional evidence in support of a heterolysis triggered by a deprotonation process of the triplet excited state ^{3}**5***, we have computed (i) the acidity of ^{3}**5*** and (ii) the potential energy surface (PES) describing the heterolytic fragmentation of the anion ^{3}**5**$^-$, generating the carbene intermediate ^{3}**5-C** and bromide anion in ACN solution. The reactivity of ^{3}**3-C** with H-donors and molecular oxygen is well-documented,[3] but our product distribution analysis reveals also a reactivity with aromatics. Therefore we also decided to investigate the reactivity of ^{3}**5-C** with pyrrole and pyridine.

Triplet State Acidity. We have evaluated the thermochemistry of the deprotonation step of ^{3}**5***, computing its pK_a in aqueous solution at PCM-UB3LYP/6-31+G(d,p) level of theory, using UAHF radii. Geometries and energies of **5**, ^{3}**5***, and its related anion ^{3}**5**$^-$ allowed the calculation of ^{3}**5*** pK_a using the isodesmic reaction in Scheme 6 and the ground state pK_a of **5** [p$K_{a,exp}$ (**5**) = 9.23][18] by eq 2, in order to cancel computational systematic errors.

$$pK_a(^3\mathbf{5}^*) = pK_{a,exp}(\mathbf{5}) + \Delta G(^3\mathbf{5}^*)/2.303RT \qquad (2)$$

$\Delta G(^3$**5***$)$ is the reaction Gibbs energy for the proton transfer equilibrium in Scheme 6 (-6.8 kcal mol^{-1}), which has been computed in aqueous solution at U(R)B3LYP/6-31+G(d,p) level of theory using PCM solvation model, and UAHF radii.

The resulting pK_a for ^{3}**5*** (pK_a 4.2) suggests that the lowest triplet excited state is more acid than the singlet ground state but also less acid than the singlet excited state of phenols.[19] Therefore the deprotonation process generating the anion in its triplet state should be thermodynamically favored in the presence of a base (Et_3N), particularly in neat ACN.

Heterolytic Fragmentation Process. With the aim to evaluate the reactivity of the 6-Br-naphtholate anion in its triplet state (^{3}**5**$^-$), we computationally explored the potential energy surface (PES) for its heterolytic fragmentation, generating the intermediate ^{3}**5-C** and bromide anion in ACN solution (Scheme 7).

The anion in the lowest triplet state ^{3}**5**$^-$, the TS **TS-**^{3}**5**$^-$, and the intermediate ^{3}**5-C** have been optimized at PCM-R(U)B3LYP/6-31+G(d,p) level of theory in ACN solution, using both UA0 and UHF radii. The **TS-**^{3}**5**$^-$ is very "early" (Figure 5), exhibiting an

(17) (a) Das, T. N.; Neta, P. *J. Phys. Chem. A* **1998**, *102*, 7081–7085. (b) Das, P. K.; Encinas, M. V.; Steenken, S.; Scaiano, J. C. *J. Am. Chem. Soc.* **1981**, *103*, 4162–4166.

(18) (a) Rosenberg, J. L.; Brinn, I. M. *J. Chem. Soc., Faraday Trans. 1* **1976**, *72*, 448–452. (b) Rosenberg, J. L.; Brinn, I. M. *J. Phys. Chem.* **1972**, *76*, 3558–3562.

(19) (a) Gao, J.; Li, N.; Freindorf, M. *J. Am. Chem. Soc.* **1996**, *118*, 4912–4913. (b) Granucci, G.; Hynes, J. T.; Millie, P.; Tran-Thi, T.-H. *J. Am. Chem. Soc.* **2000**, *122*, 12243–12253. (c) Jacoby, C.; Boehm, M.; Vu, C.; Ratzer, C.; Schmitt, M. *Chem. Phys. Chem.* **2006**, *7*, 448–454.

SCHEME 7. Generation of the Carbene ^{3}5-C Investigated at R(U)B3LYP/6-31+G(d,p) Level of Theory in ACN Solution

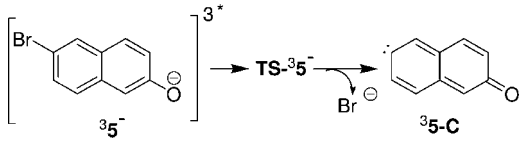

TABLE 3. Gibbs Free Energy (G, in hartree), Thermal Correction to Gibbs Free Energy (δG, in hartree), and Activation Gibbs Free Energy ($\Delta G^{\ddagger}$, in kcal mol^{-1}) for the Heterolysis of the C−Br Bond in the 6-Br-Naphtholate Anion Triplet State (^{3}5$^-$), in ACN at PCM-R(U)B3LYP/6-31+G(d,p) Level with Both UA0 and UAHF Radii

stationary points	G_{CH_3CN}	δG	$\Delta G^{\ddagger}$
^{3}**5**$^-$	−3031.717083[a]	0.087107[a]	4.36[a]
	−3031.717072[b]		5.93[b]
TS-^{3}**5**$^-$	−3031.708401[a]	0.085366[a]	
	−3031.705893[b]		

[a] PCM-UB3LYP/6-31+G(d,p), UA0 radii. [b] PCM-UB3LYP/6-31+G(d,p), UAHF radii.

almost planar structure with the C−Br bond undergoing heterolytic cleavage stretched from 1.984 Å in ^{3}**5**$^-$ to 2.131 Å in **TS-**^{3}**5**$^-$ [in ACN, at PCM-R(U)B3LYP/6-31+G(d,p) level of theory].

The activation free energy for the heterolytic fragmentation in ACN is very low, being only 4.4 kcal mol^{-1}. Similar results have also been obtained using UAHF radii ($\Delta G^{\ddagger} = 5.9$ kcal mol^{-1}; Table 3). The reaction path from **TS-**^{3}**5**$^-$ downhill to the intermediate ^{3}**5-C** followed by IRC calculations at PCM-B3LYP/6-31+G(d,p) level, in ACN, demonstrated the direct connection between the **TS-**^{3}**5**$^-$ to the final intermediate ^{3}**5-C** and bromide anion, which form a complex (at 3.018 Å C$_6$−Br distance) lying 8.8 kcal mol^{-1} below the reactants. These data unequivocally suggest that the heterolysis of the C−Br bond, triggered by the deprotonation of the triplet excited state, is kinetically the most accessible reaction pathway for the triplet excited state ^{3}**5***. The triplet state of the intermediate ^{3}**5-C**, resulting from the heterolysis of ^{3}**5**$^-$, displays a planar geometry, while the singlet (^{1}**5-C**) exhibits the C$_6$ slightly bent out of plane and puckered (Figure 5). ^{3}**5-C** is much more stable than ^{1}**5-C** by 18.8 and 20.6 kcal mol^{-1}, in ACN solution and in gas phase, respectively.

Comparison between Carbenes ^{3}3-C and ^{3}5-C. Grabner, analyzing the orbitals of ^{3}**3-C** (at AM1 level of theory), suggested that the p$_z$ orbital of C$_4$ can be considered a frontier orbital, strongly localized and singly occupied (Scheme 8).

The other nearly degenerative orbital can be constructed from the C$_4$ p$_x$ orbital in conjugation with the π orbitals of the enone system.[3a] The intermediate ^{3}**5-C** exhibits [at UB3LYP/6-31+G(d,p) level] a very similar singly occupied p$_z$-like orbital on C$_6$ and another one almost degenerate, which can be constructed from the C$_6$ p$_x$ orbital in conjugation with the extended π orbitals of the naphthalene aromatic system (Scheme 8). Therefore, as already suggested by Grabner,[3a] the reactivity

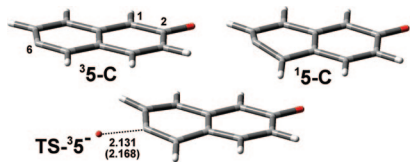

FIGURE 5. Geometries of the stationary points **TS-**^{3}**5**$^-$, ^{3}**5-C**, and ^{1}**5-C**, in acetonitrile solution at PCM-UB3LYP/6-31+G(d,p) level of theory, using both UA0 and UAHF radii (in parenthesis).

SCHEME 8. Comparison of the SOMOs for ^{3}3-C and ^{3}5-C Using Schematic Representations, Which Reveals the Pronounced Aryl Radical Nature of ^{3}5-C at C$_6$

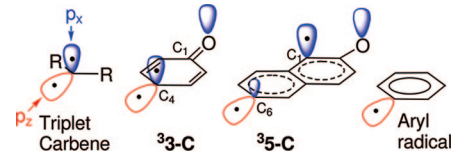

SCHEME 9. Arylation/Alkylation Reaction Mechanism Involving ^{3}5-C

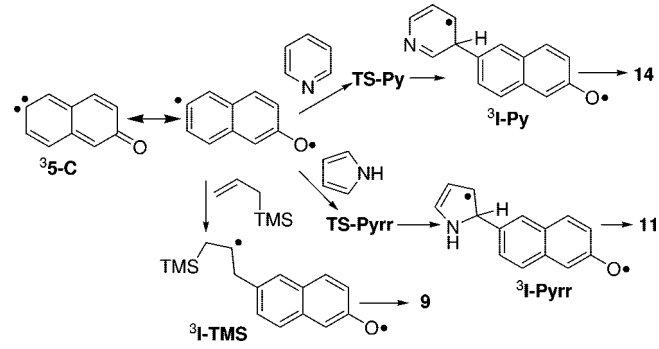

of both the intermediate ^{3}**3-C** and ^{3}**5-C** should resemble that of an aryl radical, in contrast to an aliphatic carbene, which exhibits two equivalent singly occupied p-like orbitals. In addition, the total spin density for ^{3}**5-C** is mainly localized on the C$_6$ (in the naphthalene plane) and on both the oxygen and C$_1$ atoms (orthogonal to the naphthalene plane, see Scheme 8 and Figure 6). In contrast, the total spin density for ^{3}**3-C** is mainly localized only on the C$_4$ and on the oxygen atom.

In other words, the naphthalene delocalization causes a lessening of the carbene-like character on the C$_6$ carbon. This evidence suggests that passing from ^{3}**3-C** to ^{3}**5-C** there is a further shift from a carbene-like to an aryl radical-like character. Therefore, the aryl radical nature at the C-atom should be more pronounced for ^{3}**5-C** than for ^{3}**3-C**.

Reactivity of ^{3}5-C with Pyrrole and Pyridine. We also explored the generation of the final adducts starting from the intermediate ^{3}**5-C**, investigating the triplet PES for the carbene addition to pyrrole and pyridine. The calculations have been performed in ACN solution (by PCM solvation models), in the frame of DFT, using B3LYP, PBE0, and MPWB1K functionals. We had chosen these three functionals because B3LYP is the most widely employed in organic reactivity,[11] PBE0 has been extensively used by Barone for predicting reactivity in polar media,[12] and the MPWB1K functional has been explicitly recommended by Thrular for thermochemical kinetics.[13] We have been able to localize both TSs (**TS-Py** and **TS-Pyrr**) and intermediates (^{3}**I-Py** and ^{3}**I-Pyrr**) along the radical arylation pathways (Scheme 9).

Geometries and energies (Table 4) of the stationary points in Figure 7 are very similar using the different functionals. TS geometries (**TS-Pyrr** and **TS-Py**) suggest that ^{3}**5-C** reacts as an aryl radical with only one C−C forming bond.

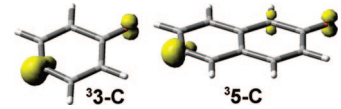

FIGURE 6. Spin density isosurfaces of ^{3}**3-C** and ^{3}**5-C**, at UB3LYP/6-31+G(d,p) level of theory, in the gas phase.

TABLE 4. Gibbs Free Energy (G, in hartree) and Activation Gibbs Free Energy ($\Delta G^{\ddagger}$, in kcal mol^{-1}) for the Radical Arylation of Pyrrole and Pyridine by ^{3}5-C, in ACN using B3LYP, PBE0, and MPWB1K Functionals with 6-31+G(d,p) Basis Set and PCM Solvation Model

stationary points	G_{CH_3CN}	$\Delta G^{\ddagger}$
^{3}5-C	−459.822409 [a]	
	−459.284591 [b]	
	−459.590222 [c]	
TS-Py	−708.118249 [a]	6.3[a]
	−707.281959 [b]	5.3[b]
	−707.751524 [c]	6.1[c]
TS-Pyrr	−670.013339 [a]	2.2[a]
	−669.222087 [b]	1.7[b]
	−669.666239 [c]	2.0[c]

[a] PCM-R(U)B3LYP/6-31+G(d,p) UA0 radii; pyrrole: −210.194536; pyridine: −248.305986. [b] PCM-R(U)PBE0/6-31+G(d,p), UAHF radii; pyrrole: −209.940134; pyridine: −248.005876. [c] PCM-R(U)MPWB1K/6-31+G(d,p), UAHF radii; pyrrole: −210.079160; pyridine: −248.171050.

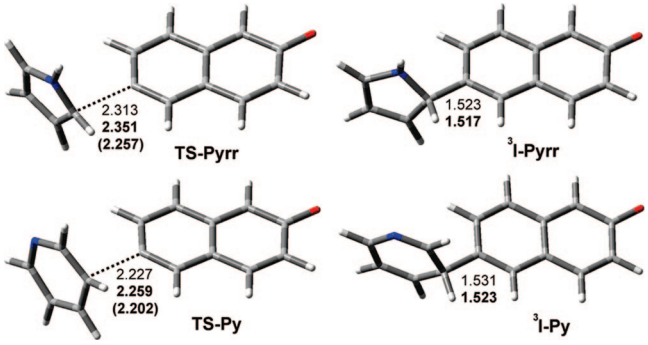

FIGURE 7. TSs (**TS-Pyrr** and **TS-Py**) and intermediates (**^{3}I-Pyrr** and **^{3}I-Py**) for the radical arylation of pyrrole and pyridine, by **^{3}5-C** using B3LYP, PBE0 (bold characters), and MPWB1K (in parenthesis) functionals and 6-31+G(d,p) basis set, in acetonitrile as solvent (modeled by PCM solvation model and UA0 radii).

The radical arylation of pyrrole by **^{3}5-C**, generating the intermediate **^{3}I-Pyrr** (Scheme 9) is an almost barrierless process, since the early **TS-Pyrr** lies 2.2 kcal mol^{-1} (Table 4) above the reactants, in ACN solution. The radical arylation of pyridine at C_3 is slightly more endoergonic, but the activation Gibbs energy in ACN is still very low (≤6.3 kcal mol^{-1}). Therefore, the radical arylation should compete efficiently with the polymerization of **^{3}5-C**.

It is interesting to stress at this point that the triplet PES lies below the singlet PES from the reactants (**^{3}5-C** + heteroaromatic) to TSs included, for the arylation of both pyrrole and pyridine. In contrast, the intermediate **I-Pyrr** is less stable in the triplet state (**^{3}I-Pyrr**) than in the singlet state (**^{1}I-Pyrr**) by at least 5.8 kcal/mol [from a single point calculation on the optimized geometry of the triplet state, at PCM-UB3LYP/6-31G(d,p) level], unlike **I-Py**, which is still more stable in the lowest triplet state (**^{3}I-Py**, by 17.7 kcal/mol). Therefore, downhill from the **TS-pyrr** there could be a triplet-singlet PES crossing point, leading to a zwitterionic intermediate in its singlet state and to the final observed product by proton transfer. Such a mechanism should be operative also for the arylation of allyltrimethylsilane, since from product distribution analysis the TMS cation loss was the only process detected.

Conclusions

In this paper we have described the photoreactivity of the triplet excited states of 6-bromonaphthols in water and in acetonitrile in the presence of Et_3N, using product distribution analysis, LFP, CV measurements, and DFT calculations in condensed phase. We have shown that, similarly to 4-chlorophenol, 6-Br-naphthol photogenerates the triplet carbenes **^{3}5-C** starting from the triplet excited state **^{3}5**. The carbene can be trapped efficiently by oxygen to give the detectable 2,6-naphthoquinone-*O*-oxide (530 < λ < 650 nm). **^{3}5** is less basic than the excited state of **1**, and unlike the 4-chlorophenols, photoheterolysis requires the deprotonation by an added amine (Et_3N). PET has been ruled out from the possible reaction mechanisms. The product distribution analysis of the photoreactions in the presence of several alkenes and aromatics, together with a DFT computational investigation, suggests that the aryl radical nature of the carbene **^{3}5-C** is more pronounced than that of Grabner's carbene **3**. Such a difference allows the achievement of a fairly efficient arylation/alkylation of aromatics and alkenes, through a radical-like pathway.

Experimental Section

Bromo-naphthol **5** and 2,6-dihydroxynaphthalene were used without further purification. The other substituted naphthols (**6**−**8**) were synthesized via standard procedures already published.[20] Compounds **10** and **16** have been identified by comparison to other authentic samples.

Procedure for Irradiation of 5 in the Presence of Pyrrole. An argon-purged solution of **5** (134 mg, 0.6 mmol), freshly distilled pyrrole (2.01 g, 30 mmol), and Et_3N (120 mg, 1.0 mmol) in 300 mL of CH_3CN was irradiated in Pyrex tubes (20 mL) for 1 h, by a multilamp reactor fitted with four 15 W lamps, with maximum emission centered at 360 nm. Chromatographic separation (cyclohexane/ethyl acetate = 7: 3), following solvent removal by vacuum concentration, gave 41 mg of **11** (83% yield) and 4 mg of **10** (4% yield).

6-(1*H*-Pyrrol-2-yl)-naphthalen-2-ol (11). Green oil. ^{1}H NMR (200 MHz, acetone-d_6): δ 6.10−6.25 (m, 1H), 6.55−6.65 (m, 1H), 6.80−6.95 (m, 1H), 7.00−7.25 (m, 2H), 7.55−7.80 (m, 3H), 8.00 (s, 1H), 8.60 (s, 1H), 10.50 (broad s, 1H). ^{13}C NMR (acetone-d_6): δ 106.7, 110.2, 110.5, 119.9, 120.1, 122.0, 124.9, 127.8, 129.4, 130.1, 130.3, 130.4, 134.7, 156.2. Anal. Calcd for $C_{14}H_{11}NO$: C, 80.36; H, 5.30; N, 6.69; O, 7.65. Found: C, 80.30; H, 5.35; N, 6.69.

General Procedure for Irradiation of 5 in the Presence of Alkenes and Pyridine. Experiments were carried out as described above using a solution of **5** (2×10^{-3} M) and Et_3N (2×10^{-3} M) after adding the traps: allyltrimethylsilane, 2,3-dimethyl-2-butene, acrylonitrile, pyridine, morpholine, and EVE ($1-5 \times 10^{-2}$ M), in acetonitrile.

6-Allylnaphthalen-2-ol (9). White crystals. Mp 90.1−90.3 °C. ^{1}H NMR (300 MHz, $CDCl_3$): δ 3.55 (d, $^3J_{H,H}$ = 6.4 Hz, 2 H), 5.13 (broad s, 1H) 5.19−5.23 (m, 2 H), 6.03−6.20 (m, 1 H), 7.00−7.20 (m, 2 H), 7.30−7.40 (m, 1 H), 7.59 (s, 1H) 7.64 (d, $^3J_{H,H}$ = 8.4 Hz, 1H), 7.72 (d, $^3J_{H,H}$ = 8.7 Hz, 1H). ^{13}C NMR ($CDCl_3$): δ 40.1, 109.3, 115.8, 117.7, 126.4, 126.5, 128.0, 129.0, 129.3, 133.1, 135.1, 137.4, 152.8. Anal. Calcd for $C_{13}H_{12}O$: C, 84.75; H, 6.57; O, 8.68. Found: C, 84.66; H, 6.67.

6-(1,1,2-Trimethylallyl)naphthalen-2-ol (12). Colorless oil. ^{1}H NMR (200 MHz, acetone-d_6): δ 1.50 (s, 9 H), 4.90 (t, $^3J_{H,H}$ = 2.0 Hz, 1 H), 5.05 (broad s, 1 H), 7.05−7.20 (m, 2 H), 7.30 (dd, $^3J_{H,H}$ = 10.0 Hz, $^3J_{H,H}$ = 2.0 Hz, 1 H), 7.60 (d, $^3J_{H,H}$ = 10.0 Hz, 1 H), 7.70 (d, $^3J_{H,H}$ = 2.0 Hz, 1 H), 7.75 (d, $^3J_{H,H}$ = 10.0 Hz, 1 H), 8.60 (s, 1 H). ^{13}C NMR ($CDCl_3$): δ 20.8, 29.0, 44.9, 109.9, 110.5, 119.5, 124.9,

(20) (a) Groves, J. T.; Viskif, P. *J. Org. Chem.* **1990**, *55*, 3628–3634. (b) Mewshaw, R. E., Jr.; Yang, C.; Manas, E. S.; Xu, Z. B.; Henderson, R. A., Jr.; Harris, H. A. *J. Med. Chem.* **2005**, *48*, 3953–3979. (c) Murphy, R. A.; Kung, H. F.; Kung, M. P.; Billings, J. *J. Med. Chem.* **1990**, *33*, 171–178. (d) Li, X.; Hewgley, J. B.; Mulrooney, C. A.; Yang, J.; Kozlowski, M. C. *J. Org. Chem.* **2003**, *68*, 5500–5511.

126.9, 127.3, 129.8, 130.7, 134.8, 143.9, 153.9, 156.4. Anal. Calcd for $C_{16}H_{18}O$: C, 84.91; H, 8.02; O, 7.07. Found: 84.88; H, 8.09.

3-Bromo-3-(6-hydroxynaphthalen-2-yl)propionitrile (13). Colorless oil. ^{1}H NMR (300 MHz, acetone-d_6): δ 3.50 (d, $^3J_{H,H}$ = 8.0 Hz, 2 H), 4.50 (t, $^3J_{H,H}$ = 7.7 Hz, 1 H), 5.10 (s broad, 1 H), 7.00−7.15 (m, 2 H), 7.25−7.40 (m, 1 H), 7.60−7.90 (m, 3 H). ^{13}C NMR (acetone-d_6): δ 27.2, 42.7, 109.3, 116.9, 118.4, 127.2, 127.2, 128.4, 128.7, 128.8, 129.7, 134.1, 153.8. Anal. Calcd for $C_{13}H_{10}BrNO$: C, 56.55; H, 3.65; Br, 28.94; N, 5.07; O, 5.79. Found: C, 56.63; H, 3.69; Br, 28.79; N, 5.11.

6-Pyridin-3-yl-naphthalen-2-ol (14). White crystals. Mp 250−252 °C. ^{1}H NMR (300 MHz, DMSO-d_6): δ 7.10 (m, 2 H), 7.60 (dd, $^3J_{H,H}$ = 7.9 Hz, $^3J_{H,H}$ = 4.8 Hz, 1 H), 7.80−7.90 (m, 3 H), 8.20 (s, 1 H), 8.30 (d, $^3J_{H,H}$ = 7.9 Hz, 1 H), 8.60 (d, $^3J_{H,H}$ = 4.8 Hz, 1 H), 9.00 (s, 1 H), 9.90 (broad s, 1 H). ^{13}C NMR (DMSO-d_6): δ 108.1, 118.9, 124.1, 124.5, 125.5, 126.6, 127.4, 129.6, 130.0, 133.9, 135.1, 135.9, 145.8, 146.2, 155.6. Anal. Calcd for $C_{15}H_{11}NO$: C, 81.43; H, 5.01; N, 6.33; O, 7.23. Found: 81.33; H, 5.10; N, 6.01.

General Procedure for Irradiation of 5 in the Presence of 1,4-Dimethoxybenzene. An argon-purged solution of **5** (134 mg, 0.6 mmol), 1,4-dimethoxybenzene (0.828 g, 20 mmol), and Et_3N (120 mg, 1.0 mmol) in 300 mL of CH_3CN was irradiated in Pyrex tubes (20 mL) for 1 h by a multilamp reactor fitted with four 15 W lamps, with maximum emission centered at 360 nm. Chromatographic separation (cyclohexane/ethyl acetate = 9:1), following solvent removal by vacuum concentration, gave 34 mg of **10** (20% yield) and 60 mg of **15** (70% yield).

6-(2,5-Dimethoxy-phenyl)-naphthalen-2-ol (15). Colorless oil. ^{1}H NMR (300 MHz, $CDCl_3$): δ 3.79 (s, 3 H), 3.85 (s, 3 H), 5.04 (bs, 1 H, -OH), 6.90 (dd, $^3J_{H,H}$ = 8.9 Hz, $^3J_{H,H}$ = 3.0 Hz, 1 H), 6.98 (d, $^3J_{H,H}$ = 8.9 Hz, 1 H), 7.02 (d, $^3J_{H,H}$ = 3.0 Hz, 1 H), 7.12 (dd, $^3J_{H,H}$ = 8.8 Hz, $^3J_{H,H}$ = 2.5 Hz, 1 H), 7.18 (d, $^3J_{H,H}$ = 2.5 Hz, 1 H), 7.66 (dd, $^3J_{H,H}$ = 8.5 Hz, $^3J_{H,H}$ = 1.7 Hz, 1 H), 7.72 (d, $^3J_{H,H}$ = 8.5 Hz, 1 H), 7.80 (d, $^3J_{H,H}$ = 8.8 Hz, 1 H), 7.92 (bs, 1 H). ^{13}C NMR (300 MHz, $CDCl_3$): δ 55.74, 56.32, 109.19, 112.72, 112.95, 116.78, 117.70, 125.67, 127.86, 128.47, 128.77, 130.01, 131.63, 133.54, 133.72, 150.88, 153.36, 153.74. Anal. Calcd for $C_{18}H_{16}O_3$: C, 77.12; H, 5.75; O, 17.12. Found: C, 77.20; H, 5.63.

Procedure for Irradiation of 8 in the Presence of Pyrrole in Acetonitrile. A N_2-purged solution of **8** (160 mg, 0.6 mmol), freshly distilled pyrrole (2.01 g, 30 mmol) and Et_3N (122 mg, 1.1 mmol) in 300 mL of CH_3CN was irradiated in Pyrex tubes (20 mL) for 1 h, by a multilamp reactor fitted with four 15 W lamps, with maximum emission centered at 360 nm. Reverse phase chromatographic separation on RP-C18 silica (MeOH/H_2O = 6:4), following solvent removal by vacuum concentration, gave 59 mg of **16** (52% yield) and 43 mg of **17** (20% yield).

3-Hydroxy-7-(1*H*-pyrrol-2-yl)naphthalene-2-carboxylic Acid Triethylammonium Salt (17). Pale green crystals. Mp 95−97.2 °C. ^{1}H NMR (300 MHz, CD_3OD): δ 1.20 (t, $^3J_{H,H}$ = 7.3 Hz, 9 H), 3.10 (q, $^3J_{H,H}$ = 7.3 Hz, 6 H), 4.90 (s, 1 H), 6.15 (m, 1 H), 6.50 (m, 1 H), 6.85 (m, 1 H), 7.10 (s, 1 H), 7.55 (d, $^3J_{H,H}$ = 8.7 Hz, 1 H), 7.70 (dd, $^3J_{H,H}$ = 8.7 Hz, $^3J_{H,H}$ = 1.7 Hz, 1 H), 7.90 (s, 1 H), 8.40 (s, 1 H). ^{13}C NMR (CD_3OD): δ 9.4, 48.0, 106.6, 110.4, 111.1, 120.2, 122.7, 122.8, 126.5, 127.5, 129.3, 129.9, 132.8, 133.4, 137.0, 158.8, 175.7. Anal. Calcd for $C_{21}H_{26}N_2O_3$: C, 71.16; H, 7.39; N, 7.90; O, 13.54. Found: C, 70.87; H, 7.49, N, 7.79.

Procedure for Irradiation of 8 in the Presence of Pyridine in Aqueous Acetonitrile. A N_2-purged solution of **8** (161 mg, 0.6 mmol), freshly distilled pyridine (5.0 g. 4.8 mL, 63 mmol), and Na_2CO_3 (1.30 g, 12.3 mmol) in 300 mL of CH_3CN/H_2O = 1:1 was irradiated in Pyrex tubes (20 mL) for 1 h by a multilamp reactor fitted with four 15 W lamps, with maximum emission centered at 360 nm. Reverse phase chromatographic separation on RP-C18 silica (MeOH/H_2O = 6:4), following solvent removal by vacuum concentration, gave 64 mg of **16** (57% yield) and 36 mg of **18** (21% yield).

3-Hydroxy-7-pyridin-3-yl-naphthalene-2-carboxylic Acid Sodium Salt (18). Yellow solid. Mp > 250 °C. ^{1}H NMR (200 MHz, DMSO): δ 4.30 (s, 1 H), 7.40 (s, 1 H), 7.65−7.85 (m, 1 H), 7.80−8.00 (m, 2 H), 8.30−8.50 (m, 2 H), 8.70 (m, 2 H), 9.15 (s, 1 H). ^{13}C NMR: δ 109.6, 119.6, 122.7, 124.1, 125.5, 127.1, 128.6, 131.2, 131.7, 133.9, 135.1, 136.4, 145.8, 146.2, 158.8, 175.7. Anal. Calcd for $C_{16}H_{10}NNaO_3$: C, 66.90; H, 3.51; N, 4.88; Na, 8.00; O, 16.71. Found: C, 66.79; H, 3.59; N, 4.83.

Electrochemical Measurements. Cyclic voltammetries (CV) were performed using a BAS EPSILON for Electrochemistry equipped with a glassy carbon disk electrode and a Ag/AgCl/KCl (4 M KCl saturated with AgCl) reference electrode, in degassed acetonitrile using Bu_4NPF_6 0.1 M, sweep rate from 100 to 1500 mV s^{-1}. All potentials in the text are reported vs Ag/AgCl/KCl (4 M KCl saturated with AgCl).

Methods and Computation Details. All calculations were carried out using Revision D.02 of the Gaussian 03 program package.[21] The structures of the triplet excited state of **^{3}5*** and the intermediates (**^{3}5$^-$**, **^{3}5-C**, **^{1}5-C**, **^{3}I-Py**, and **^{3}I-Pyrr**) and the transition states (**TS-^{3}5$^-$**, **TS-Py**, and **TS-Pyrr**) were fully optimized in the gas phase and in acetonitrile solution using the B3LYP,[11] PBE0,[12] and MPWB1K[13] functionals, with the 6-31+G(d,p) basis set. It is known that diffuse functions are mandatory for a reliable evaluation of anion energies and H-bonding, and in our reactive system an anionic character is present in both the triplet state **^{3}5$^-$** and also at the oxygen atom in **^{3}5-C**. Thermal contributions (ΔG) to activation free energy were computed from B3LYP/6-31+G(d,p) structures and harmonic frequencies, by using the harmonic oscillator approximation and the standard expressions for an ideal gas in the canonical ensemble at 298.15 K and 1 atm. The optimization of the stationary points in the solvent bulk were calculated via the self-consistent reaction field (SCRF) method using PCM as implemented in the D.02 version of Gaussian 03.[21] Such a model includes the nonelectrostatic terms (cavitation, dispersion, and repulsion energy) in addition to the classical electrostatic contribution. The cavities within the solvent are composed by interlocking spheres centered on non-hydrogen atoms with both UA0 and UAHF radii.

Acknowledgment. Financial support from Pavia University ("Fondo FAR 2007") and "Consorzio CINMPIS" is gratefully acknowledged. We also thank CICAIA (Modena University) and CINECA (Bologna University) for computer facilities.

Supporting Information Available: ^{1}H NMR, and ^{13}C NMR spectra for the adducts **9**, **11**−**15**, **17**, and **18**, electrochemical data (Figures S1 and S1a), Cartesian coordinates of reactants and intermediates (**^{3}5$^-$**, **^{3}5-C**, **^{1}5-C**, **^{3}I-Py** and **^{3}I-Pyrr**) and the transition states (**TS-^{3}5$^-$**, **TS-Py**, and **TS-Pyrr**) at the R(U)B3LYP/6-31+G(d,p) R(U)PBE0/6-31+G(d,p) and MPWB1K/6-31+G(d,p) level (gas phase and acetonitrile solution). This material is available free of charge via the Internet at http://pubs.acs.org.

JO802374R

(21) Frisch, M. J.; Trucks, G. W.; Schlegel, H. B.; Scuseria, G. E.; Robb, M. A.; Cheeseman, J. R.; Montgomery, J. A., Jr.; Vreven, T.; Kudin, K. N.; Burant, J. C.; Millam, J. M.; Iyengar, S. S.; Tomasi, J.; Barone, V.; Mennucci, B.; Cossi, M.; Scalmani, G.; Rega, N.; Petersson, G. A.; Nakatsuji, H.; Hada, M.; Ehara, M.; Toyota, K.; Fukuda, R.; Hasegawa, J.; Ishida, M.; Nakajima, T.; Honda, Y.; Kitao, O.; Nakai, H.; Klene, M.; Li, X.; Knox, J. E.; Hratchian, H. P.; Cross, J. B.; Bakken, V.; Adamo, C.; Jaramillo, J.; Gomperts, R.; Stratmann, R. E.; Yazyev, O.; Austin, A. J.; Cammi, R.; Pomelli, C.; Ochterski, J. W.; Ayala, P. Y.; Morokuma, K.; Voth, G. A.; Salvador, P.; Dannenberg, J. J.; Zakrzewski, V. G.; Dapprich, S.; Daniels, A. D.; Strain, M. C.; Farkas, O.; Malick, D. K.; Rabuck, A. D.; Raghavachari, K.; Foresman, J. B.; Ortiz, J. V.; Cui, Q.; Baboul, A. G.; Clifford, S.; Cioslowski, J.; Stefanov, B. B.; Liu, G.; Liashenko, A.; Piskorz, P.; Komaromi, I.; Martin, R. L.; Fox, D. J.; Keith, T. Al-Laham, M. A. Peng, C. Y.; Nanayakkara, A.; Challacombe, M.; Gill, P. M. W.; Johnson, B.; Chen, W.; Wong, M. W.; Gonzalez, C.; Pople, J. A. *Gaussian 03, Revision D.02*; Gaussian, Inc.: Wallingford, CT, 2004.